Disulfide bond formation involves a quinhydrone-type charge–transfer complex

James Regeimbal*, Stefan Gleiter*, Bernard L. Trumpower†, Chang-An Yu‡, Mithun Diwakar*, David P. Ballou§, and James C. A. Bardwell*¶

Departments of *Molecular, Cellular, and Developmental Biology and §Biological Chemistry, University of Michigan, Ann Arbor, MI 48109-1048; †Biochemistry Department, Dartmouth Medical School, Hanover, NH 03755; and ‡Department of Biochemistry and Molecular Biology, Oklahoma State University, Stillwater, OK 74078

Communicated by Elizabeth Anne Craig, University of Wisconsin Medical School, Madison, WI, September 17, 2003 (received for review July 14, 2003)

The chemistry of disulfide exchange in biological systems is well studied. However, the detailed mechanism of how oxidizing equivalents are derived to form disulfide bonds in proteins is not clear. In prokaryotic organisms, it is known that DsbB delivers oxidizing equivalents through DsbA to secreted proteins. DsbB becomes reoxidized by reducing quinones that are part of the membrane-bound electron-transfer chains. It is this quinone reductase activity that links disulfide bond formation to the electron transport system. We show here that purified DsbB contains the spectral signal of a quinhydrone, a charge–transfer complex consisting of a hydroquinone and a quinone in a stacked configuration. We conclude that disulfide bond formation involves a stacked hydroquinone–benzoquinone pair that can be trapped on DsbB as a quinhydrone charge–transfer complex. Quinhydrones are known to be redox-active and are commonly used as redox standards, but, to our knowledge, have never before been directly observed in biological systems. We also show kinetically that this quinhydrone-type charge–transfer complex undergoes redox reactions consistent with its being an intermediate in the reaction mechanism of DsbB. We propose a simple model for the action of DsbB where a quinhydrone-like complex plays a crucial role as a reaction intermediate.

Many extracellular proteins require the formation of one or more disulfide bonds to achieve their correct tertiary structure. Because of the importance of disulfides in the folding of many proteins, the process of disulfide formation in biological systems has been studied extensively. The DsbA-DsbB oxidation-reduction pathway is responsible for *de novo* disulfide formation in *Escherichia coli*, and has been heavily investigated by several groups for almost 15 years. As a result, much is known about this system. For recent reviews, see refs. 1 and 2.

DsbA is a 21-kDa periplasmic protein that is a member of the thioredoxin superfamily. DsbA has a very reactive active-site high-redox-potential disulfide that can readily transfer oxidizing equivalents to a wide variety of substrate proteins (1, 2). When DsbA donates its disulfide bond to a secreted target protein, DsbA is released in a reduced state. To function as a catalyst, DsbA must be reoxidized. This reoxidation is accomplished by its partner protein, DsbB (3). DsbB is a 20-kDa inner-membrane protein that is predicted to have four transmembrane helices and two periplasmic loops (4). DsbB has four conserved cysteines that are required for activity; the first pair is located in the N-terminal periplasmic loop and the second pair is located in the C-terminal periplasmic loop (5). The overall reaction that DsbB catalyzes is the formation of a disulfide bond within DsbA and the reduction of a membrane-bound quinone. This reaction provides a pathway for the oxidative power of the electron transport system to be used to form a disulfide within DsbA and ultimately within secreted proteins (3, 6, 7). The mechanism of DsbB begins with the reduction of a quinone to form a disulfide bond within the DsbB protein itself. This action is followed by two disulfide–dithiol exchange reactions, one within DsbB, and the second to form a disulfide in DsbA. The exact mechanism of disulfide exchange within DsbB is a matter of controversy that has recently been reviewed (8). A number of different models have been proposed by us and by others (9–12), partly based on genetic evidence and on rather indirect thiol trapping experiments. These thiol-trapping experiments apparently resulted in inaccurate measurements of the redox potentials of the disulfides within DsbB, and, therefore, introduced uncertainty about the flow of electrons within DsbB. However, very recently, Grauschopf *et al.* (13) reported fluorescence experiments that directly measured the redox potentials of the active site cysteines of DsbB. These results and kinetic experiments provide strong evidence that is consistent with the original model of DsbB action proposed by Ito and coworkers (11, 14). In this model, a disulfide first forms between the N-terminal pair of cysteines within DsbB by quinone reduction. This disulfide is then transferred to the C-terminal pair of cysteines within DsbB, and then finally to DsbA. Keeping the controversy alive, however, is another very recent paper (15), where the stability of oxidized DsbB was shown to be greater than that of reduced DsbB, but not the other way around, as predicted by the Ito model (11, 14).

Disulfide-interchange reactions have been extensively studied in many systems, and much of the work on DsbB has been focused on determining the exact sequence of the thiol-disulfide interchange reactions within DsbB and between DsbB and DsbA. However, far less is known about the more interesting and novel reaction carried out by DsbB, where it generates a disulfide, *de novo*, by the reduction of quinones. It is this quinone reductase activity that links disulfide-bond formation to the electron transport system and makes DsbB a key disulfide-generating enzyme in E. *coli* (6, 7). It is, thus, of great interest to investigate the quinone reductase mechanism of DsbB.

After purification, DsbB is found to have the quinone, ubiquinone-40, (Q-8) bound (7). The quinone-binding properties of DsbB have been investigated, and DsbB is known to have at least one strong quinone-binding site that apparently involves Arg-48 and a region containing residues 91–97 (7, 16, 17). We previously showed that DsbB functions as a very efficient quinone reductase and is capable of catalyzing the oxidation of DsbA through quinone reduction rapidly and specifically. The apparent k_{cat}/K_m value for the DsbB-catalyzed reaction between quinone and reduced DsbA is $4{\cdot}10^6\ M^{-1}{\cdot}s^{-1}$ (7).

Purified DsbB is strikingly purple. We have concluded that the purple color in DsbB is due to a bound quinhydrone-type charge–transfer complex. This finding is based on similarities between the spectral properties of DsbB and quinhydrone charge–transfer complexes, as well as analysis of the kinetics of DsbB catalysis. Quinhydrones, which are charge–transfer complexes of a hydroquinone and a quinone in a stacked configu-

BIOCHEMISTRY

Abbreviations: Q-8, ubiquinone-40; DM, *n*-dodecyl-β-D-maltopyranoside; Q_0C_{10}, 2,3-dimethoxy-5-methyl-6-decyl-1,4-benzoquinone; $H_2Q_0C_{10}$, 2,3-dimethoxy-5-methyl-6-decyl-1,4-hydroquinone.

¶To whom correspondence should be addressed. E-mail: jbardwel@umich.edu.

ration, are redox-active isoforms of quinone that are commonly used as redox standards, but this is the first report of which we are aware that quinhydrones form in biological systems.

Methods

Fermentation and Protein Purification. The DsbB coding sequence was cloned into the isopropyl β-D-thiogalactoside (IPTG)-inducible expression vector, pQE70, to generate the overexpression plasmid, pWM76. Wild-type DsbB contains four conserved cysteines (DsbB[CCCC]). Three derivatives were prepared: DsbB[SSCC] and [CCSS] where the N-terminal or C-terminal cysteines are substituted with serines, and a DsbB mutant, DsbB[SSSS], in which all four cysteines were replaced. His-tagged versions of wild-type DsbB and these mutant variants were introduced into JR6. This strain is a *dsbB*::*kan* insertion null mutant derived from the standard expression strain, BL21.

Cells were fermented in a New Brunswick Scientific Bioflo 4500 fermentor/bioreactor in an initial volume of 14 liters of 50 g/liter yeast extract, containing 0.5 g/liter ammonium chloride, 2% glycerol, 2.76 mM $MgSO_4$, 50 mM K_2HPO_4, and 600 μg/ml ampicillin supplemented with 0.8 g of thiamine. Cells were grown to an OD_{600} of ≈30 and induced with either 100 or 500 μM IPTG for 5 h. The cells were slowly fed 3 liters of 30% yeast extract containing 25% glycerol during induction. Dissolved O_2 was maintained at 20% and pH was maintained at 7.0 during the entire fermentation. On reaching stationary phase (OD_{600} of ≈80), cells were harvested by centrifugation at 4,000 rpm in a JS-4.2 rotor for 20 min and frozen at −80°C until use. Final yields were usually 3–5 kg of wet cell paste per 14 liters of fermentation. Membrane extracts were prepared as described (6). The DsbB-His-containing membranes were solubilized in 50 mM NaP_i, pH 8.0, containing 300 mM NaCl and 5 mM 3-[(3-cholamidopropyl)dimethylammonio]-1-propanesulfonate (CHAPS) for 1.5 h at 4°C. The solubilized membranes were cleared by centrifugation at 48,000 × *g* for 1 h, filtered at 0.2 μm, and dialyzed against 20 mM Tris·HCl, pH 8.5, containing 0.1 mM CHAPS. After dialysis, the membranes were loaded onto a Q-Sepharose column equilibrated with 20 mM Tris·HCl, pH 8.5, containing 0.1 mM CHAPS. The flow-through, which contained DsbB, was first concentrated and then diluted into 50 mM NaP_i, pH 8.0, containing 300 mM NaCl and 2% *n*-dodecyl-β-D-maltopyranoside (DM). This partially purified DsbB was then fully purified as described (6). Reduced DsbA was purified essentially as described (18).

Absorbance Spectra. All absorbance spectra were measured at room temperature with a Beckman DU 640 spectrophotometer or with a Hi-Tech SF-61 stopped-flow spectrophotometer.

MS. Samples for electrospray ionization MS were prepared by freeze-drying followed by resuspension in methanol. To extract organic cofactors, hexane was added and the sample was vortexed. After separation of the two phases, the hexane phase was removed and evaporated under vacuum. The sample was dissolved in dichloromethane and diluted with a solution containing 90% methanol and 0.2 mM NaCl. The solution was directly infused into the electrospray source with a flow rate of 30 μl/min.

MS was performed with a Micromass Autospec Ultima magnetic sector instrument. Scan range was *m/z* 1,800 to *m/z* 75 at a rate of 8 sec/decade. The spectrometer was calibrated by using a mixture of polyethylene glycols.

Enzyme Kinetics. Stopped-flow studies were carried out by using a Hi-Tech Scientific SF-61 single-mix stopped-flow spectrophotometer controlled by Kinetic Instruments software. DsbB[CCCC] and reduced DsbA were mixed in the stopped-flow instrument to final concentrations of 75 and 750 μM, respectively. The reactions were monitored at 505 nm.

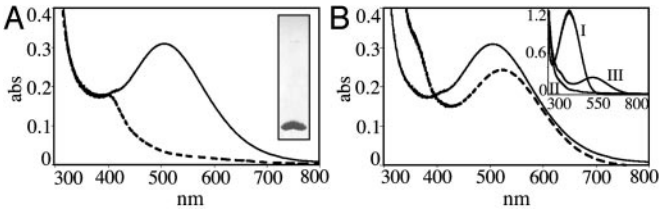

Fig. 1. (*A*) Absorbance spectra of DsbB[CCCC] (wild-type) and DsbB[SSSS]. After purification, DsbB[CCCC] has a brilliant purple color, whereas DsbB[SSSS] is yellow. Absorbance spectra of DsbB[CCCC] (solid line) and DsbB[SSSS] (dashed line) illustrate this difference and show that DsbB[CCCC] has a broad band with its maximum at 505–510 nm. This broad band is not present in the spectrum of DsbB[SSSS]. Spectra of DsbB[CCCC] and DsbB[SSSS] were recorded by using 100 μM protein in 20 mM Hepes (pH 7.5), 20 mM NaCl, and 0.02% DM at room temperature. (*Inset*) The purity of DsbB[CCCC] used in this study. By scanning this SDS/PAGE gel, the purity was determined to be ≈96%. (*B*) Overlay spectra of DsbB[CCCC] and quinhydrone. Shown are the spectra of 100 μM DsbB[CCCC] (solid line) in 20 mM Hepes, pH 7.5, containing 20 mM NaCl, 0.02% DM, and of quinhydrone (dashed line) prepared by making a 1:1 ratio mixture of 2.5 mM $H_2Q_0C_{10}$ and 2.5 mM Q_0C_{10} in 100% ethanol. (*Inset*) The spectra of various Q_0C_{10} species in 100% ethanol. Q_0C_{10} (benzoquinone) (line I) is yellow in color, whereas $H_2Q_0C_{10}$ (hydroquinone) (line II) is colorless. Quinhydrone (line III), generated by mixing 2.5 mM $H_2Q_0C_{10}$ and 2.5 mM Q_0C_{10} in a 1:1 ratio, has a brilliant purple color. All spectra of the quinones in the absence of protein were measured at room temperature in 100% ethanol.

***In Vitro* Formation of Quinhydrone in Solution.** The decylubiquinone, 2,3-dimethoxy-5-methyl-6-decyl-1,4-benzoquinone (Q_0C_{10}) (Sigma), was resuspended in 100% ethanol. The hydroquinone, 2,3-dimethoxy-5-methyl-6-decyl-1,4-hydroquinone ($H_2Q_0C_{10}$), was generated by adding a small amount of solid $NaBH_4$ to Q_0C_{10}. The quinhydrone was generated by mixing one part of $H_2Q_0C_{10}$ with one part of Q_0C_{10}.

Results and Discussion

Absorbance Spectra and MS Analysis of Purified DsbB. There is a distinct difference in color between purified DsbB (DsbB[CCCC]) and various inactive mutants of DsbB that lack some or all of the conserved cysteines (DsbB[CCSS], DsbB[SSCC], and DsbB[SSSS]). Wild-type DsbB[CCCC] has a brilliant purple color, whereas DsbB[CCSS], DsbB[SSCC], and DsbB[SSSS] are all yellow. The absorbance spectrum of DsbB[CCCC] shows a broad band with a maximum at ≈510 nm, which is absent from the spectrum of DsbB[SSSS] (Fig. 1*A*) or any of the other cysteine mutants we constructed (data not shown). It is unlikely that the purple color found in the wild-type DsbB protein was due to the presence of an impurity. First, this preparation of DsbB is 96% pure, as determined by scanning of the SDS/PAGE gel (Fig. 1*A Inset*). A very minor contaminating protein present on overloaded gels was sequenced and found to be either OmpF or PhoE; both are colorless, highly homologous outer membrane proteins. Second, purple proteins are exceedingly rare. The best-known example is bacteriorhodopsin, a protein that is present in purple photosynthetic bacteria, but not in *E. coli*. To our knowledge, no other purple protein has been reported in *E. coli*.

We previously identified (7) the quinone that remains bound to DsbB during the purification process as Q-8 by comigration with ubiquinone-5, ubiquinone-10, Q-8, and ubiquinone-50 standards on a reverse phase C8-HPLC column. The most obvious possibility was that the purple color of purified DsbB is somehow related to this bound Q-8 cofactor. To obtain additional evidence that the quinone bound to DsbB is indeed Q-8, we performed electrospray ionization MS analysis on our purified purple DsbB. This analysis was performed, in part, because several quinone species, such as quinhydrone charge–transfer complexes, the deprotonated form of hydroxyquinone, and

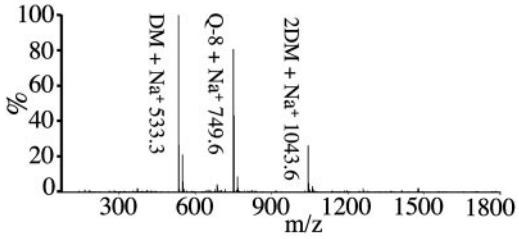

Fig. 2. Electrospray ionization MS (ESI-MS) of DsbB reveals that it contains a bound coenzyme, Q-8. DsbB was extracted with hexane and prepared for ESI-MS as described in *Methods*. The spectrum revealed three dominant peaks. DM ($+Na^+$), with an m/z of 533.3, corresponds to the sodium adduct of DM, the detergent used in this study. 2DM ($+Na^+$) corresponds to a detergent dimer with an m/z of 1043.6. Q-8 ($+Na^+$) corresponds to the mass of a coenzyme Q-8 sodium adduct with an m/z of 749.6.

rhodoquinone, are known to have a purple color (19). We favored the involvement of Q-8 in a charge–transfer complex because Q-8 is known to be the most abundant quinone present in *E. coli* membranes under aerobic growth conditions, and because it is known to bind DsbB (7). Rhodoquinone and hydroxyquinones, in contrast, are much less likely candidates. Rhodoquinone is found in Rhodobacter and mitochondria, but, as far as we are aware, has not been found in *E. coli*. Hydroxyquinones are synthetic analogues of quinones that have not yet been isolated from biological systems (20–22). As shown in Fig. 2, two major compounds were observed in our MS analysis of purified wild-type DsbB after extraction with methanol and hexane, a molecular mass of 533.3 Da and a molecular mass of 749.6 Da. These correspond very well to the mass of a single-Na^+ adduct of DM [formula weight (FW) 533.3], the detergent used to solubilize and reconstitute DsbB, and the Na^+ adduct of coenzyme Q-8 (FW 749.5). In addition, we see a companion peak of unknown origin that is 16 Da larger than 533.3, and a peak that is 16 Da larger than 749.6 Da, which probably correspond to the addition of a single oxygen atom to DM and Q-8, respectively. The peak at 1043.6 corresponds to the Na^+ adduct of a dimer of two DM molecules (FW 1043.6). No other major peaks are seen. In summary, the only cofactor that hexane extraction removed from DsbB was coenzyme Q-8.

Absorbance Spectra of Various Redox States of Q_0C_{10}. We suspected that the purple color in DsbB was due to a charge–transfer complex known as a quinhydrone (Fig. 3) because quinhydrones are purple (23). Quinhydrones consist of a reduced quinone interacting with an oxidized quinone through ring stacking (Fig. 3). In the presence of light, an electron from the reduced hydroquinone (donor) is then transferred to the oxidized benzoquinone (acceptor), giving the quinhydrone its very characteristic purple color (Fig. 3) (23).

We investigated whether a reconstituted quinhydrone is formed between oxidized ubiquinone, Q_0C_{10}, and its reduced hydroquinone form, $H_2Q_0C_{10}$, and whether this complex has a similar

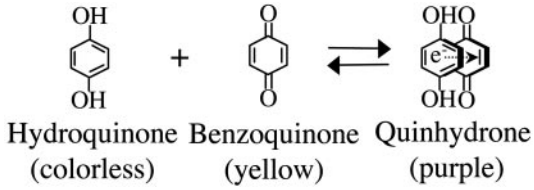

Fig. 3. A schematic representation of quinhydrone formation. Hydroquinone and benzoquinone stack onto each other in a 1:1 ratio. In the presence of light, an electron is donated from the hydroquinone to the benzoquinone, forming a charge–transfer complex to give the characteristic purple color

spectrum to the cofactor that is bound to DsbB. We chose Q_0C_{10} because it is a commonly used ubiquinone species and it is known to be a good substrate for DsbB (6). Q-8, the quinone found bound to *E. coli* DsbB, is not commercially available and is known to be very insoluble in aqueous solutions. Fig. 1*B Inset* shows absorbance spectra of the various redox states of Q_0C_{10}. Oxidized Q_0C_{10} (benzoquinone) is yellow with a broad band with a maximum at 405–415 nm (Fig. 1*B Inset*, line I). A small shoulder at this wavelength is present in the spectra of the yellow cysteine mutants of DsbB[CCSS], DsbB[SSCC], and DsbB[SSSS] (Fig. 1*A* and data not shown). Reduced Q_0C_{10} (hydroquinone or $H_2Q_0C_{10}$) was generated by adding a small amount of solid $NaBH_4$ to Q_0C_{10}. As shown by its absorbance spectrum, $H_2Q_0C_{10}$ is colorless (Fig. 1*B Inset*, line II). A quinhydrone charge–transfer complex between $H_2Q_0C_{10}$ and Q_0C_{10} was generated by mixing $H_2Q_0C_{10}$ and Q_0C_{10} to a final concentration of 2.5 mM each. On incubation overnight, the solution turned purple, which is a diagnostic indicator for the formation of quinhydrone (23). Fig. 1*B Inset* shows the absorbance spectrum of the quinhydrone, which has a broad band with a maximum at ≈520 nm (line III). In addition, there is a small shoulder at 370 nm due to unreacted benzoquinone and hydroquinone.

The spectrum of the quinhydrone in ethanol (dashed line) is very similar to the spectrum of DsbB[CCCC] (solid line) (Fig. 1*B*). The minor difference in the absorption maximum and spectrum shape may be due partly to the environment, because one cofactor was present in a protein/detergent micellar environment, whereas the other was in an ethanol solution. In addition, there is a difference in the length of the hydrocarbon chain between Q-8, which has a 40-carbon hydrophobic tail, and Q_0C_{10}, which has a 10-carbon hydrophobic tail. Finally, the presence of unreacted benzoquinone and hydroquinone in the alcoholic solution may distort the spectrum slightly. Despite all of these potentially confounding variables, the two spectra are very similar. Wild-type DsbB (DsbB[CCCC]) thus appears to have a spectrum characteristic of a quinhydrone, which is bound to the protein. It is likely that the previously documented quinone (7) participates in forming the charge–transfer complex described here. The possibility that the color derives from a semiquinone state (which would have an unpaired electron) is unlikely, because the purple DsbB[CCCC] is EPR-silent (data not shown).

Oxidized quinones can form colored quinhydrone-like charge–transfer complexes with tyrosine residues (23). To investigate whether the charge-transfer spectrum of DsbB could be due to the interaction of a quinone with tyrosine, we incubated equimolar quantities of *p*-benzoquinone with tyrosine. A reddish-brown complex was formed with maximal absorption peaks at ≈360 nm and ≈455 nm (data not shown), which is very different from the spectrum of DsbB. This result does not completely exclude the possibility that a tyrosine-quinone charge–transfer complex imparts the color to DsbB, because the protein environment could influence the spectral characteristics of such a complex. However, if a tyrosine in DsbB were to interact directly with a quinone to form a charge–transfer complex that was important in the enzymatic reaction mechanism, we would expect that tyrosine would be highly conserved throughout evolution. There are six tyrosines in DsbB, five of which are not at all conserved. The remaining tyrosine, Y46, is only poorly conserved. Thus, it is unlikely that any of these tyrosines play a vital catalytic role. In addition, purified DsbB Y46A retains the purple color throughout purification (data not shown). Although we cannot exclude the possibility that the color in DsbB[CCCC] is due to a charge–transfer complex between benzoquinone and a tyrosine present in DsbB, we consider it unlikely.

All of the inactive cysteine mutants of DsbB, we examined, namely DsbB[SSSS], DsbB[CCSS], and DsbB[SSCC] are yellow,

indicating that the mutations interfered with the formation of the purple color. We suggest that the yellow color of these proteins is due to the quinones being bound in the oxidized state to these variants of DsbB. By contrast, wild-type DsbB[CCCC] appears to have a bound quinhydrone-type charge–transfer complex, which suggests that the active-site cysteines are required for quinhydrone formation. Quinhydrones are known to be redox-active. Because of their well defined redox properties, they are commonly used in calibrating oxidation-reduction potential (redox) electrodes (Sensorex, Garden Grove, CA) and have been used in pH electrodes (24). However, to our knowledge, this is the first clear evidence that quinhydrones play a role in protein function.

The Putative Quinhydrone in DsbB[CCCC] Responds to pH in the Same Manner as Bona Fide Quinhydrone. Quinhydrones are pH-sensitive. Thus, acidifying the ethanolic solution of quinhydrone causes the solution to turn from purple to yellow within seconds. It seems likely that at alkaline pH, the hydroquinone is deprotonated and thereby becomes a better charge-transfer donor. Making this solution alkaline restored the purple color within seconds, and the spectrum was identical to the initial spectrum of the quinhydrone (data not shown). Because the initial formation of the purple color was very slow (see above), this rapid regeneration of the purple color on making the solution alkaline indicates that the ring stacking of the quinhydrone is not destroyed by pH change. Rather, the acid pH seems to prevent charge transfer.

We next tested whether the apparent quinhydrone in DsbB[CCCC] had a similar pH sensitivity and reversibility to that of quinhydrones as shown above. The storage buffer of DsbB[CCCC] is 20 mM Hepes, pH 7.5, containing 20 mM NaCl and 0.02% DM, and the protein is purple under these conditions. We dialyzed DsbB[CCCC] against a phosphate buffer at pH 6.0 and found that the color changed to a faint yellow. When the same protein was dialyzed against a phosphate buffer at pH 8.0, the purple color was restored. Titration of the pH with phosphate buffer revealed that the purple-to-yellow color transition occurred with a pK_a of ≈6.8. By pH 6.0, the solution was a faint yellow. This result showed that the apparent quinhydrone in DsbB[CCCC] has a reversible response to pH similar to that of quinhydrones.

The Quinhydrone in DsbB Is Redox-Sensitive and Bleaches in Response to DsbA. Quinhydrones are known to be sensitive to redox agents (25). We therefore compared the sensitivity of free quinhydrone derived from a mixture of $H_2Q_0C_{10}$ and Q_0C_{10} to that of the putative Q-8 quinhydrone in DsbB to a variety of redox agents. Solid $NaBH_4$ as well as a 5-fold excess of DTT both caused the purple color of DsbB and the free quinhydrone to bleach. A 5-fold excess of ascorbic acid or H_2O_2, on the other hand, had no effect on the purple color of either DsbB or free quinhydrone. This finding indicated that both quinhydrones have redox potentials somewhat lower than that of ascorbate and cannot be oxidized by H_2O_2.

Because the quinhydrone in DsbB could be reduced to a colorless compound by reducing agents such as DTT, we tested whether the *in vivo* substrate of DsbB, namely reduced DsbA, could also cause the reduction of the putative quinhydrone in DsbB, thereby bleaching its color. We monitored the reaction of DsbB with an excess of reduced DsbA by stopped-flow spectrophotometry. The reaction between reduced DsbA and DsbB[CCCC] was carried out aerobically at pH 8.0. DsbB and reduced DsbA were combined to final concentrations of 75 and 750 μM, respectively, and the reaction was monitored at 505 nm. As shown in Fig. 4, the purple color in DsbB decreased rapidly after reduced DsbA was added, indicating that the quinhydrone is indeed being reduced in the reaction. Fig. 4 *Inset* shows the spectra before and after the reaction. There are several phases in the overall reaction, but most of the absorbance

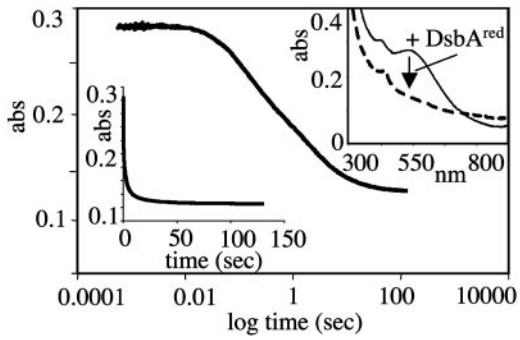

Fig. 4. Stopped-flow analysis of the rapid oxidation of DsbA by DsbB. DsbB and reduced DsbA were mixed in the stopped-flow spectrophotometer to final concentrations of 75 and 750 μM, respectively, and the reaction was monitored at 505 nm. Reactions were carried out in 50 mM NaP_i containing 300 mM NaCl and 0.02% DM at pH 8.0 and 25°C. The kinetic trace is shown in both a linear and logarithmic time scale. (*Inset*) The spectra before and after the reaction.

decrease occurs in phases of 0.8 and ≈6 s^{-1}. We previously measured (7) the V_{max} of the oxidation of DsbA by DsbB to be 5 s^{-1}. This finding makes the second phase of the reaction shown in Fig. 4 kinetically competent to support catalytic turnover. The rapid loss of the purple color on addition of DsbA shows that the quinhydrone is consumed when the physiological reductant of DsbB is added, providing strong evidence for its involvement in the enzymatic reaction.

When one compares the spectrum of a 0.1-mM solution of DsbB protein with that of a 1:1 ratio mixture of 2.5 mM hydroquinone and 2.5 mM benzoquinone (Fig. 1*B*), one sees that the amplitudes of the two spectra are very similar at 510 nm, implying a large difference in apparent extinction coefficients of the quinhydrone bound to DsbB and quinhydrone in solution. It is known that in solution, quinhydrones are largely dissociated into quinone and hydroquinone (26). The Nernst equation ($\ln K_{eq} = nF\varepsilon^\circ/RT$) and the standard redox potentials of unsubstituted quinone and quinhydrone allows one to calculate the equilibrium constant for the reaction $QNH <-> Q + H_2Q$, and thus the proportion of unsubstituted quinone present in the quinhydrone form in solution. The redox potential of unsubstituted quinone is 99 mV (27). The redox potential of quinhydrone is pH-dependent, conforming to the equation $E = U_{st} - 0.1984 \cdot (273.16 + t) \cdot$ pH, where U_{st} is the standard redox potential at temperature, t (699.7 mV at 25 °C), giving a redox potential of 167.3 mV at 25°C and pH 9. Combining these two half-reactions, we obtain a potential of 68.3 mV for the equilibrium $QNH <-> Q + H_2Q$. By using the Nernst equation with this potential, we obtain $K_{eq} = 2.06 \times 10^2$ M indicating that at pH 9, <1% of quinone in solution is expected to be present as quinhydrone. These redox potentials are for unsubstituted quinones; unfortunately, no redox potential is available for the quinone present in the DsbB, Q-8 because of its very poor solubility in water. The redox potential of the Q_0C_{10} quinhydrone is also unknown. If these values are similar to that of unsubstituted quinone, as seems likely, then Q-8 and Q_0C_{10} quinhydrones should also be largely dissociated into quinone and hydroquinone in solution. The large difference in the apparent extinction coefficients between the quinhydrone present in DsbB and that of quinhydrone in solution, implies that the DsbB protein environment acts to stabilize the quinhydrone form. Consistent with this result, denaturation of DsbB by addition of SDS destroys the purple color (data not shown).

It has been proposed that a quinhydrone may be an intermediate in the mechanism of the cytochrome bc1 complex. In this model, two quinones occupy the Q_o-binding site, Q_{os} and Q_{ow}.

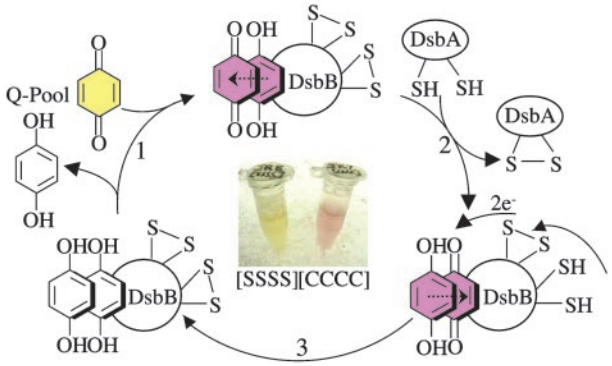

Fig. 5. A working model for the reaction cycle for the quinone reductase activity of DsbB. The quinone reductase activity of DsbB involves two quinones: a prosthetic quinone, which remains bound to DsbB, and a more transient quinone. The prosthetic and transient quinones are initially reduced, as shown in the leftmost diagram in the figure. An oxidized quinone derived from the quinone pool replaces the transient reduced quinone (step 1). The resident reduced quinone transfers electrons to the transient quinone through a quinhydrone complex, as shown at the top. The reoxidation of DsbA results in reduction of the C-terminal disulfide in DsbB (step 2), which undergoes dithiol-disulfide exchange with the N-terminal cysteines. The newly formed N-terminal dithiol reduces the prosthetic quinone (step 3). Because the two reduced quinones do not form a stable complex, the transient hydroquinone is exchanged with an oxidized quinone (step 1). At this state, DsbB can enter a new cycle of catalysis to reoxidize another molecule of DsbA. (*Inset*) At the center is a photograph of 120 μM DsbB[CCCC] and DsbB[SSSS], illustrating the striking color difference between the wild-type and the cysteineless mutant of DsbB. For wild-type DsbB purified in the absence of DsbA, the reaction cycle is interrupted at step 2 and it accumulates the purple quinhydrone species shown at the top. The cysteineless mutant of DsbB is unable to transfer disulfides within DsbB and thus accumulates the quinone bound to it in a yellow oxidized form.

Q_{os} binds with higher affinity and may function as a prosthetic group, whereas Q_{ow} binds more transiently. Bifurcated electron transport is thought to originate at these two quinones through a quinhydrone charge-transfer intermediate. However, the quinhydrone has never been directly observed and its possible involvement remains controversial (28–31). Here we show evidence that a quinhydrone is found in DsbB. Because the quinhydrone is present in wild-type DsbB, and absent from the inactive variants that lack at least one pair of cysteines, it is reasonable to believe that the active-site cysteines are involved in quinhydrone formation. Kinetic results suggest that the quinhydrone is involved in the reaction mechanism of DsbB.

Model of DsbB Action. We propose a model where a stacked quinone system in DsbB may function similarly to the proposed quinhydrone in the cytochrome bc1 complex. DsbB is known to have at least one high-affinity quinone site (7). In our model depicted in Fig. 5, one hydroquinone would function as a prosthetic group. This prosthetic hydroquinone would act as a docking site for an oxidized quinone, supplied by the electron transport chain (step 1 in Fig. 5). The resident prosthetic hydroquinone transfers electrons to the transient quinone through π-π electron transfer. This stacked quinone configuration can be trapped as a quinhydrone charge–transfer complex as shown at the top of Fig. 5. DsbA also acts to reduce the C-terminal cysteines in DsbB (step 2). Next, the reduction of the prosthetic quinone occurs, as shown in the intermediate at the bottom in Fig. 5. This quinone reduction results in disulfide bond formation within DsbB (step 3). Two reduced quinones in a stacked configuration (as depicted in the left intermediate in Fig. 5) are known to be less stable than a quinhydrone charge–transfer complex (23). This unstable ring stacking would allow the transient, reduced quinone to rapidly dissociate from DsbB and be replaced by an oxidized quinone, supplied by the oxidized quinone pool, completing the catalytic cycle (step 1). The disulfide bonds formed in DsbB by quinone reduction are passed on to DsbA and ultimately oxidize secreted proteins. The involvement of a quinhydrone in the mechanism of DsbB ensures efficient electron transport and quinone exchange. It is possible that the quinhydrone has some semiquinone character that promotes electron transfer from the dithiols.

Reaction intermediates are often difficult to trap in enzymatic systems. Why did we apparently succeed in trapping a never-before-observed intermediate simply by purifying DsbB away from DsbA at high pH? We suggest that this purple quinhydrone intermediate accumulates in purified DsbB for the following three reasons: First, the catalytic cycle is interrupted on purification of DsbB because no DsbA is present to serve as a reductant. In the absence of an appropriate electron donor. DsbB accumulates with all of its cysteines present in a disulfide-bonded form and its quinones in a quinhydrone form. Second, the quinhydrone complex is more stable than either of the two other proposed quinone intermediates, namely two oxidized benzoquinones stacked together or two reduced hydroquinones stacked together. Third, the purple color of quinhydrones is more visible at high pH. Indeed, it is possible to destroy the purple color of the quinhydrone in DsbB[CCCC] by incubating at pH 6.0, probably because the anionic phenolate is protonated. Curiously, the pH optimum for DsbB is pH 6.0 (32). This finding is rather peculiar for an enzyme involved in thiol-disulfide exchange reactions, which are usually more favorable at pH values that are close to the pK_a of cysteine, pH 9. It may be that the unusual pH optimum of DsbB is due to the involvement of the quinhydrone in the reaction mechanism. Shifting to a more basic pH would stabilize the quinhydrone intermediate, thus diminishing the catalytic efficiency of DsbB.

We thank Dr. Ursula Jakob, Dr. Charlie Yocum, and Jonathan Pan for useful discussions, and Dr. James Windack for performing the MS analyses. This work was supported by National Institutes of Health Grants GM057039 (to J.C.A.B.), GM11106 (to D.P.B.), GM20379 (to B.L.T.), and GM30721 (to C.-A.Y.). J.R. was supported by National Institutes of Health National Research Service Award #2-T32-GM007544-26 from the National Institute of General Medical Sciences. S.G. was supported by Deutsche Akademie der Naturforscher Leopoldina Grant BMBF-LPD 9901/8-79.

1. Collet, J. F. & Bardwell, J. C. (2002) *Mol. Microbiol.* **44,** 1–8.
2. Kadokura, H., Katzen, F. & Beckwith, J. (2003) *Annu. Rev. Biochem.* **72,** 111–135.
3. Bardwell, J. C., Lee, J. O., Jander, G., Martin, N., Belin, D. & Beckwith, J. (1993) *Proc. Natl. Acad. Sci. USA* **90,** 1038–1042.
4. Jander, G., Martin, N. L. & Beckwith, J. (1994) *EMBO J.* **13,** 5121–5127.
5. Kobayashi, T., Kishigami, S., Sone, M., Inokuchi, H., Mogi, T. & Ito, K. (1997) *Proc. Natl. Acad. Sci. USA* **94,** 11857–11862.
6. Bader, M., Muse, W., Ballou, D. P., Gassner, C. & Bardwell, J. C. (1999) *Cell* **98,** 217–227.
7. Bader, M. W., Xie, T., Yu, C. A. & Bardwell, J. C. (2000) *J. Biol. Chem.* **275,** 26082–26088.
8. Vinson, V. (2002) *Science* **296,** 1767.
9. Inaba, K. & Ito, K. (2002) *EMBO J.* **21,** 2646–2654.
10. Kadokura, H. & Beckwith, J. (2002) *EMBO J.* **21,** 2354–2363.
11. Kishigami, S., Kanaya, E., Kikuchi, M. & Ito, K. (1995) *J. Biol. Chem.* **270,** 17072–17074.
12. Regeimbal, J. & Bardwell, J. C. (2002) *J. Biol. Chem.* **277,** 32706–32713.
13. Grauschopf, U., Fritz, A. & Glockshuber, R. (2003) *EMBO J.* **22,** 3503–3513.
14. Kobayashi, T. & Ito, K. (1999) *EMBO J.* **18,** 1192–1198.
15. Otzen, D. E. (2003) *J. Mol. Biol.* **330,** 641–649.
16. Kadokura, H., Bader, M., Tian, H., Bardwell, J. C. & Beckwith, J. (2000) *Proc. Natl. Acad. Sci. USA* **97,** 10884–10889.
17. Xie, T., Yu, L., Bader, M. W., Bardwell, J. C. & Yu, C. A. (2002) *J. Biol. Chem.* **277,** 1649–1652.
18. Wunderlich, M. & Glockshuber, R. (1993) *Protein Sci.* **2,** 717–726.

19. Sanjust, E., Rinaldi, A. C., Rescigno, A., Porcu, M. C., Alberti, G., Rinaldi, A. & Finazzi-Agro, A. (1995) *Biochem. Biophys. Res. Commun.* **208,** 825–834.
20. Takamiya, S., Matsui, T., Taka, H., Murayama, K., Matsuda, M. & Aoki, T. (1999) *Arch. Biochem. Biophys.* **371,** 284–289.
21. Miyadera, H., Hiraishi, A., Miyoshi, H., Sakamoto, K., Mineki, R., Murayama, K., Nagashima, K. V., Matsuura, K., Kojima, S. & Kita, K. (2003) *Eur. J. Biochem.* **270,** 1863–1874.
22. Palsdottir, H., Lojero, C. G., Trumpower, B. L. & Hunte, C. (2003) *J. Biol. Chem.* **278,** 31303–31311.
23. Slifkin, M. A. (1971) *Charge Transfer Interactions of Biomolecules* (Academic, London).
24. Aquinobinag, C., Pigram, P. J., Lamb, R. N. & Alexander, P. W. (1994) *Anal. Chim. Acta* **291,** 65–73.
25. Wetzler, R., Muller, L. & Gottlich, P. (1977) *Z. Phys. Chem. (Leipzig)* **258,** 528–532.
26. Vogel, A. I. (1956) in *A Textbook of Practical Organic Chemistry* (Addison–Wesley, Reading, MA), 3rd Ed., p. 745.
27. Wardman, P. (1989) *J. Phys. Chem. Ref. Data* **18,** 1637–1755.
28. Brandt, U. (1996) *FEBS Lett.* **387,** 1–6.
29. Crofts, A. R., Guergova-Kuras, M., Kuras, R., Ugulava, N., Li, J. & Hong, S. (2000) *Biochim. Biophys. Acta* **1459,** 456–466.
30. Ding, H., Moser, C. C., Robertson, D. E., Tokito, M. K., Daldal, F. & Dutton, P. L. (1995) *Biochemistry* **34,** 15979–15996.
31. Bartoschek, S., Johansson, M., Geierstanger, B. H., Okun, J. G., Lancaster, C. R., Humpfer, E., Yu, L., Yu, C. A., Griesinger, C. & Brandt, U. (2001) *J. Biol. Chem.* **276,** 35231–35234.
32. Bader, M., Muse, W., Zander, T. & Bardwell, J. (1998) *J. Biol. Chem.* **273,** 10302–10307.